Revista Brasileira de Ensino de Física, vol. 45, e20230019 (2023)
www.scielo.br/rbef
DOI: https://doi.org/10.1590/1806-9126-RBEF-2023-0019

Articles

On the spacing distributions in the spin-1/2 XX chain

Diego Luis González[*1], Juan David Álvarez Cuartas[1], T. L. Einstein[2]

[1]Universidad del Valle, Departamento de Física, 25360, Cali, Colombia.
[2]University of Maryland, Department of Physics, 20742, College Park, USA.

Received on January 20, 2023. Accepted on March 27, 2023.

We provide a pedagogical calculation of the first two spacing distribution for a spin-1/2 XX chain in the presence of an external magnetic field. The results obtained from analytical expressions are compared with those from extensive quantum Monte Carlo simulations. The results obtained for the spacing distributions are used to describe the magnetic behavior of the system and contrasted with the standard analysis based on quantities such as the average energy, magnetization, and susceptibility. Finally, the equivalence between the analytical expressions for the spacing distributions provided by the second quantization formalism and those from the inter-particle distribution method is illustrated. As shown, the spacing distributions can be used as pedagogical examples of the use of the second quantization formalism in introductory courses of quantum statistical mechanics. Additionally, these distributions can be calculated easily from quantum Monte Carlo simulation and, therefore, can be used to illustrate this numerical method.
Keywords: Emptiness distribution, spin chain, Wigner surmise, spacing distribution functions.

1. Introduction

Two of the main tools presented in courses on quantum statistical mechanics to deal with interacting many-particle quantum systems are the second quantization formalism and the quantum Monte Carlo (QMC) method [1–11]. Thus, one of the challenges in teaching this topic is finding physical systems where these tools can easily be applied, and therefore, can be used as examples [1–8, 12, 13]. From a pedagogical perspective, an example must illustrate the nature, usefulness and scope of the methods but at the same time be accessible for an upper-level introductory course.

The XX spin chain in the presence of a magnetic field h is an integrable system and one of the simplest quantum systems displaying long-range correlations along with the associated large fluctuations. It clearly has the minimal dimensionality and number of continuous degrees of freedom per site. Therefore, it is a good starting point to begin the study of quantum interacting many-particle systems [14–19]. The XX spin chain is described by the Hamiltonian

$$\hat{\mathcal{H}} = J\sum_{j=1}^{N}\left(\hat{S}_j^x\hat{S}_{j+1}^x + \hat{S}_j^y\hat{S}_{j+1}^y\right) - 2h\sum_{j=1}^{N}\hat{S}_j^z, \quad (1)$$

where J is the coupling constant between adjacent spins, h is an external magnetic field and N the total number of spins (lattice sites). As usual, $\hat{S}_j^i$ is an operator that gives the projection of the spin in direction $i = x\,, y$ and z for the lattice site j.

From the partition function of the XX spin chain, many physical quantities can be calculated analytically, such as the free energy, magnetization, susceptibility, and heat capacity [1–3, 14]. The magnetic behavior of the system can be understood from the analysis of these macroscopic quantities. Thus, it is not surprising that the XX spin chain is often chosen to illustrate the useful of the second quantization formalism and the QMC method [11, 14, 20–22]. Besides the macroscopic quantities mentioned above, there are other quantities that can also be used to describe the behavior of spin chain and to illustrate the scope of these tools. One of them is a special correlation function called Emptiness Formation Probability (EFP), E_n, which is the probability of finding an up-string with length n

$$E_n = \left\langle \prod_{j=1}^{n}\left(\hat{S}_j^z + \frac{\hat{I}}{2}\right)\right\rangle, \quad (2)$$

where $\hat{I}$ is the identity operator. A major advantage of E_n is that, from its distribution one can calculate the scaled domain-length distribution function, $p^{(0)}(\ell)$ [15–19]. The magnetic behavior of the spin chain can be understood via the results obtained for $p^{(0)}(\ell)$. It is well known [14–16] that an interesting regime appears as $2\,h$ approaches J from below: consecutive domains of spins parallel to the field are separated from each other by a single spin pointing in the opposite direction. In this regime, it is useful to map the spin system into an equivalent system of interacting particles. In this analogy

*Correspondence email address: diego.luis.gonzalez@correounivalle.edu.co

the minority spins are represented by particles, while the spins parallel to the field by empty sites. In the context of classical systems of interacting particles, E_n is the probability to find an empty segment (without particles) of length n. We can define another quantity that also provides information about the structure formed by the domains, the probability $p^{(1)}(\ell)$. By definition $p^{(1)}(\ell)$ is the probability to find two consecutive domains separated by a single spin in the opposite direction; thus, ℓ is the sum of two domain lengths plus one additional lattice site. This probability is less studied than $p^{(0)}(\ell)$ but can also be calculated analytically for the spin-1/2 XX chain albeit not be expressable in terms of E_n [23, 24].

Typically, the structure and behavior of many-particle systems are usually described in terms of pair distributions and density correlation functions. Equivalently, the spacing distributions can be used to describe the statistical behavior of one-dimensional many particle systems [2, 25–29]. Therefore, it is not surprising that they have been used to extract information in different contexts such as reaction diffusion systems, epitaxial growth, traffic flow, and random matrices. For instance, $p^{(0)}(\ell)$ can be used to extract information about the interaction potential between particles in classical one-dimensional many-particle systems [25, 30]. In the context of random matrices, the structure formed by the eigenvalues is described by the spacing distributions, allowing one to characterize the different ensembles according to the functional form of those distributions [27]. Furthermore, there is evidence [28] that several different systems can share the same $p^{(0)}(\ell)$ even thought their statistical behaviors are not equivalent. Therefore, the finest details of their behavior are contained in the higher-order spacing distributions.

We stress the methods presented here have pedagogical value. For instance, they can fruitfully supplement specialized books devoted to the study of exactly solvable one-dimensional systems [11, 14, 31]. Such books seek to illustrate the exact calculation of several quantities for complex systems. The spacing distributions of the XX spin chain are an example of these quantities which usually is not considered. Our discussion can complement the standard material presented in the books dedicated to spin chains [14, 32, 33], the spacing distributions discussed here can provide another approach to the description of the behavior of the XX spin chain. Additionally, E_n is the basis of a method called interparticle-distribution function (IPDF), widely used in the context of reaction-diffusion systems [23, 24]. Our work exemplifies how second-quantization tools are related to the IPDF method, serving as the motivation and the starting point for the use of quantum-field-theory methods in the study of reaction-diffusion systems.

This paper is organized as follows: In the second section, we briefly present the model and the transformation used to diagonalize the Hamiltonian. A brief discussion of the magnetic behavior of the system is provided through results for the average energy, magnetization, and susceptibility. In the third section we calculate $p^{(0)}(\ell)$ and $p^{(1)}(\ell)$ for the XX spin chain. In the fourth section, we compare the analytical and numerical results for $p^{(0)}(\ell)$ and $p^{(1)}(\ell)$ produced by the second-quantization formalism and QMC, respectively. Finally, we use our results for the spacing distributions to discuss the magnetic behavior of the spin chain, as well as the pedagogical value of these calculations.

2. Model Description

Consider a chain along the z axis of N spins-1/2 with nearest-neighbor interactions in the presence of an external magnetic field h parallel to this z axis. The system is described by the Hamiltonian given in Eq. (1). Periodic boundary conditions are imposed, i.e., $\hat{S}^j_{N+1} = \hat{S}^j_1$ with $j = x, y$ or z. It is well know that this Hamiltonian can be diagonalized by using the Jordan-Wigner (JW) transformation [34], see Appendix A. Note well that the JW transformation maps the spin system onto an equivalent system of free fermions. The diagonalized form of the Hamiltonian is

$$\hat{\mathcal{H}} = \sum_q \epsilon_q \, \hat{c}^\dagger_q \hat{c}_q - h \, \hat{N}, \tag{3}$$

where the dispersion relation is given by $\epsilon_q = 2h - J\cos(q)$; $\hat{c}_q$ and $\hat{c}^\dagger_q$ are fermionic annihilation and creation operators, respectively. The density of fermions (down-spins) on the lattice is given by $\rho = N_F/N = \cos^{-1}(2h/J)/\pi$. It is illustrative to plot ϵ_q for different values of h. As shown in Fig. 1, for $h = 0$ the Fermi wavevector is given by $k_F = \pi/2$. However, as h increases k_F decreases, implying that the number of fermions decreases. For $h > J/2$ the Fermi sea disappears; the absence of fermions means that all spins are parallel to the field.

The energy of the ground state per particle, i.e., the average energy per particle at $T = 0$, is given by

$$\begin{aligned} \mathcal{E}_g &= \langle gs| \hat{\mathcal{H}} |gs\rangle \\ &= -h + \frac{1}{2\pi}\int_{-\pi\rho}^{\pi\rho} dq \, (2\,h - J\cos q) \\ &= -h(1-2\rho) - \frac{J}{\pi}\sin(\pi\,\rho)\,, \end{aligned} \tag{4}$$

where $|gs\rangle = \prod_{q=-k_F}^{k_F} \hat{c}^\dagger_q |\varnothing\rangle$ and $|\varnothing\rangle$ is the vacuum state. In Eq. (4) we use the fact that, in the thermodynamic limit ($N, N_F \to \infty$ with $\rho = N_F/N$ finite and fixed), the sum over q_l can be replaced by an integral over q according to $(1/N)\sum_l \to \int dq/(2\pi)$. From Eq. (4) at $T = 0$, for $h \geq J/2$ we have $\rho = 0$ and $\mathcal{E}_g = -h$. In contrast, for $h \to 0$, $\rho \to 1/2$, $\mathcal{E}_g \to -J/\pi$ and the number of spins up and down are equal. For non-zero temperature the thermal fluctuations must be considered. In order to do that, we must calculate the partition function of the system in the canonical ensemble, $\mathcal{Z}_N(\beta)$. The details of

 DOI: https://doi.org/10.1590/1806-9126-RBEF-2023-0019

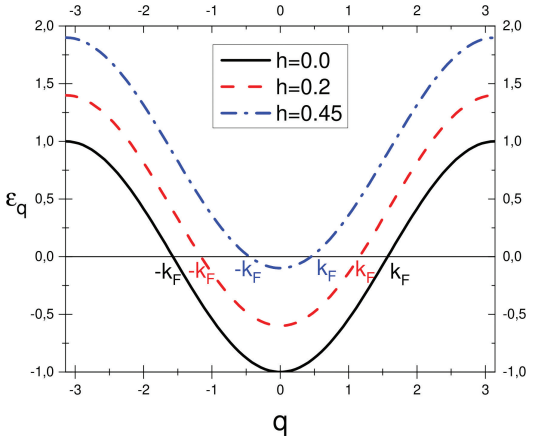

Figure 1: Behavior of ϵ_q for different values of h with $J = 1$. Here and henceforth we take $k_B = 1$ and $J = 1$ for the numerical evaluation of all quantities. The Fermi wavevector tends to zero as h gets close to $J/2$ implying the disappearance of the "down" spins.

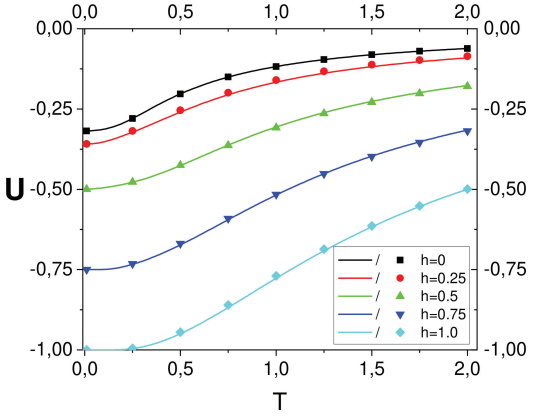

Figure 2: Energy as function of T for different values of h. Continuous lines corresponds to Eq. (6) while dots to the results obtained from QMC. For $T = 0$ the internal energy reduces to Eq. (4) while for large T the energy takes the form $\mathcal{U} \approx -\beta(h^2 + J^2/8)$.

the calculation are shown in Appendix B. The explicit form of $\mathcal{Z}_N(\beta)$ is

$$\mathcal{Z}_N(\beta) = z^{-N/2} \prod_{l=1}^{N} \left(1 + z e^{f(q)}\right), \tag{5}$$

with $q = 2\pi l/N$. As usual, in the thermodynamic limit the average energy per spin, $\mathcal{U}$, can be obtained from [1–8, 14]

$$\mathcal{U} = -h + \int_{-\pi}^{\pi} \frac{dq}{2\pi} \frac{\epsilon(q) e^{-\beta\epsilon(q)}}{1 + e^{-\beta\epsilon(q)}}. \tag{6}$$

For $T = 0$, the internal energy coincides with the ground state energy $\mathcal{E}_g$, and as T increases, $\mathcal{U}$ approaches zero, see Fig. (2). In the limit of high temperatures ($k_B T \gg J - 2h$), the parameter β is small and the internal energy reduces to $\mathcal{U} \approx -\beta(h^2 + J^2/8)$.

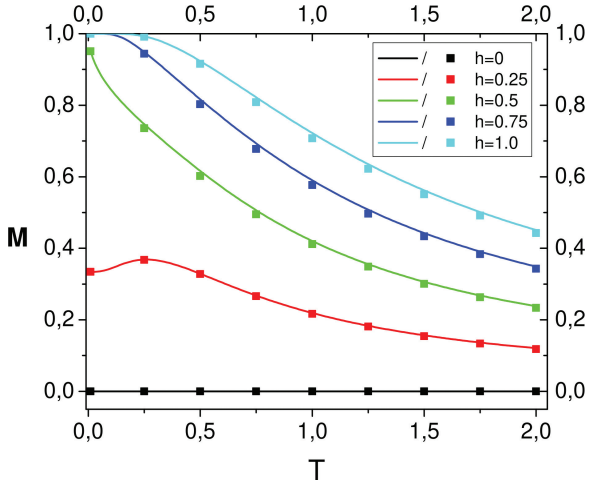

Figure 3: Magnetization as function of T for different values of h. Continuous lines correspond to Eq. (7) while dots to the results obtained from QMC. For $h = 0$ the magnetization is zero for all T. In the case $h > 0$ the magnetization is not zero for finite T but tends to zero as $T \to \infty$.

For the QMC simulation we follow the algorithm proposed by Sandvik based on a stochastic series expansion with operator-loop update [20–22]. In the simulation 500,000 MCS were used to reach equilibrium, with $N = 512$, $k_B = 1$ and $J = 1$. In all figures, continuous lines correspond to the analytic expression while dots to the numerical results obtained from a QMC simulation.

The free energy per site can be calculated straightforward from $\mathcal{Z}_N(\beta)$ and can be used to calculate the magnetization per spin

$$\mathcal{M} = 1 - \int_{-\pi}^{\pi} \frac{dq}{\pi} \frac{e^{\beta J \cos(q)}}{e^{2\beta h} + e^{\beta J \cos(q)}} \tag{7}$$

The numerical and analytical results for $\mathcal{M}$ are shown in Fig. 3. As expected, for $h = 0$ the magnetization is zero for any value of T. For $T = 0$ and $h > 0.5$ the magnetization is equal to one because all the spins are parallel to the field. For $T = 0$ and $0 < h < 0.5$ the magnetization is smaller than one due to the existence of down spins. Naturally, for $T > 0$, the magnetization decreases due to the thermal fluctuations, see Fig. 3. In fact, from Eq. (7) it is easy to see that for large T, $\mathcal{M} \approx h\beta$. For $h = 0$, $\mathcal{M} = 0$ regardless the value of T because $\rho = 1/2$, and the number of spins up and down are equal.

From the above discussion, at $T = 0$ we can expect interesting behavior as $2h$ approaches to J from below. Note that in this regime small changes in h lead to large changes in $\mathcal{M}$. The susceptibility per spin, χ, gives the response of the magnetization to changes of the magnetic field. Therefore, by definition χ can be calculated from the magnetization as follows

$$\chi = \int_{-\pi}^{\pi} dq \frac{2e^{\beta(2h + J\cos(q))}}{\pi k_B T \left(e^{2\beta h} + e^{\beta J \cos(q)}\right)^2} \tag{8}$$

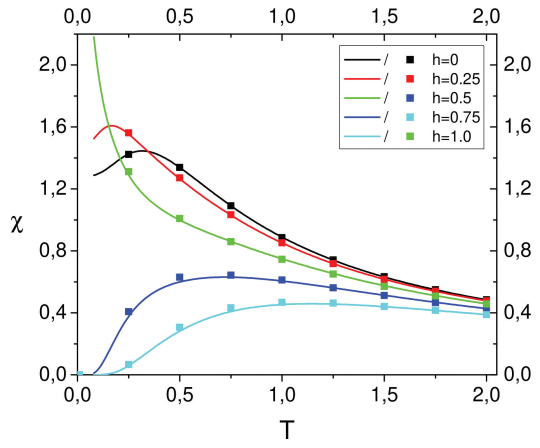

Figure 4: Susceptibility as function of T for different values of h. Continuous lines correspond to Eq. (8) while dots to the results obtained from QMC. For large T the susceptibility decreases and does not depends on h. For $T = 0$ and $h = 0.5$ an interesting behavior is found, χ diverges suggesting the presence of a critical behavior.

As seen in Fig. (4), for $h = 0.5$ the susceptibility diverges at $T = 0$. This fact suggests the existence of critical behavior associated with the crossover from the organized state $\mathcal{M} = 1$ ($2h > J$) to a disorganized state $\mathcal{M} < 1$ ($2h < J$). The magnetic behavior described in this section can be also understood in terms of the spacing distributions.

3. Spacing Distributions

In general, the spacing distributions contain information about the structure of one-dimensional systems and provide insights into the nature of the interaction between the particles. Therefore, they are often used to describe one-dimensional many-particle systems [28–30, 35, 36]. As explained earlier, the XX spin chain can be mapped onto an equivalent free fermion system, and its spacing distributions can be used to obtain information about the behavior of the spin chain.

As usual, $P^{(n)}(L)$ is the probability that for a particle at the origin we find another particle at a distance L, with the condition that there are n additional particles inside the gap between them. It is convenient to use the scaled spacing $\ell = L/\langle L\rangle$, with $\langle L\rangle$ the average of L. The scaled spacing distributions, $p^{(n)}(\ell)$, are given by

$$p^{(n)}(\ell) = \langle L\rangle\, P^{(n)}(\ell\,\langle L\rangle). \tag{9}$$

Note that we use lower case for the scaled distributions and uppercase for the unscaled ones. From their definition, it is clear that the spacing distributions are related to the pair correlation function according to $g(\ell) = \sum_{n=0}^{\infty} p^{(n)}(\ell)$. The easiest distributions to calculate analytically for the XX spin system are $p^{(0)}(\ell)$ and $g(\ell)$ [15, 17, 19, 30]. One of the objectives of the present paper is to show that $p^{(1)}(\ell)$ can also be easily calculated analytically and numerically; therefore, it can be used in courses of quantum statistical mechanics as an illustrative example. In order to accomplish this, we briefly present the standard method used to calculate $p^{(0)}(\ell)$ and then we extend it to $p^{(1)}(\ell)$. In the free fermion picture of the spin chain, each lattice site is either empty ($\circ$) or occupied ($\bullet$). Let $\mathcal{P}_{\mathcal{C}}(\mathcal{C})$ be the probability of a given configuration $\mathcal{C}$. The probabilities of both configurations for a given lattice site satisfy

$$\mathcal{P}_{\mathcal{C}}(\bullet) + \mathcal{P}_{\mathcal{C}}(\circ) = 1. \tag{10}$$

Similarly, the probabilities of the configurations of two consecutive sites are given by

$$\mathcal{P}(\bullet\bullet) + \mathcal{P}_{\mathcal{C}}(\bullet\circ) + \mathcal{P}_{\mathcal{C}}(\circ\bullet) + \mathcal{P}_{\mathcal{C}}(\circ\circ) = 1. \tag{11}$$

For an isotropic system as in this paper $\mathcal{P}_{\mathcal{C}}(\bullet\circ) = \mathcal{P}_{\mathcal{C}}(\circ\bullet)$. The key quantity required to calculate the spacing distribution $p^{(0)}(\ell)$ is the emptiness distribution E_ℓ, which is the probability to find ℓ consecutive empty lattice sites. Thus, by definition $E_2 = \mathcal{P}_{\mathcal{C}}(\circ\circ)$. On the other hand we have $\mathcal{P}_{\mathcal{C}}(\circ\circ) + \mathcal{P}_{\mathcal{C}}(\bullet\circ) = \mathcal{P}_{\mathcal{C}}(\circ)$, implying that, $\mathcal{P}_{\mathcal{C}}(\bullet\circ) = E_1 - E_2$. Thus, using these results in Eq. (11) shows that

$$\mathcal{P}_{\mathcal{C}}(\bullet\bullet) = 1 - 2E_1 + E_2. \tag{12}$$

Analogously, if we consider all the configurations of $L+1$ consecutive sites with the $L-1$ intermediate sites empty, one finds [23, 24]

$$\begin{aligned} E_{\ell-1} \;=\; & \mathcal{P}_{\mathcal{C}}(\bullet\overbrace{\circ\cdots\circ}^{L-1}\bullet) + \mathcal{P}_{\mathcal{C}}(\bullet\overbrace{\circ\cdots\circ}^{L-1}\circ) \\ & + \mathcal{P}_{\mathcal{C}}(\circ\overbrace{\circ\cdots\circ}^{L-1}\bullet) + \mathcal{P}_{\mathcal{C}}(\circ\overbrace{\circ\cdots\circ}^{L-1}\circ), \end{aligned} \tag{13}$$

which leads to

$$\begin{aligned} P^{(0)}(L) \;&=\; \mathcal{P}_{\mathcal{C}}(\downarrow\overbrace{\uparrow\cdots\uparrow}^{L-1}\downarrow) \\ &=\; \mathcal{P}_{\mathcal{C}}(\bullet\overbrace{\circ\cdots\circ}^{L-1}\bullet) \\ &=\; E_{L+1} - 2E_L + E_{L-1}, \end{aligned} \tag{14}$$

where we have used $\mathcal{P}_{\mathcal{C}}(\bullet\overbrace{\circ\cdots\circ}^{\ell-1}\circ) = E_L - E_{L+1}$. This method is well known in the context of reaction-diffusion systems as the inter-particle distribution function method (IPDF) [24, 35]. Comparing Eqs. (12) and (14) we conclude that $E_0 = 1$. Note that in order to calculate $P^{(0)}(L)$ it is only necessary to find E_n. Additionally, it is important to realize that Eq. (14) can be written equivalently by using the second quantization approach as the following average value

$$P^{(0)}(L) = \left\langle \hat{c}_0^\dagger \hat{c}_0 \prod_{j=1}^{L-1} \hat{b}_j^\dagger \hat{b}_j\, \hat{c}_L^\dagger \hat{c}_L \right\rangle, \tag{15}$$

 DOI: https://doi.org/10.1590/1806-9126-RBEF-2023-0019

where $\hat{c}_j^\dagger$ ($\hat{b}_j^\dagger$) and $\hat{c}_j$ ($\hat{b}_j$) are the fermionic (hole) creation and annihilation operators at position j, respectively. These operators are related according to $\hat{c}_j^\dagger = \hat{b}_j$ and $\hat{c}_j = \hat{b}_j^\dagger$. Taking this into account and using the fermionic commutation relations to eliminate the particle operators in Eq. (15) we find

$$P^{(0)}(L) = \left\langle \prod_{j=1}^{L-1} \hat{b}_j^\dagger \hat{b}_j \right\rangle - \left\langle \prod_{j=1}^{L} \hat{b}_j^\dagger \hat{b}_j \right\rangle - \left\langle \prod_{j=0}^{L-1} \hat{b}_j^\dagger \hat{b}_j \right\rangle + \left\langle \prod_{j=0}^{L} \hat{b}_j^\dagger \hat{b}_j \right\rangle \quad (16)$$

Comparing Eqs. (14) and (16) we can conclude that, the first term on the right side of Eq. (16) corresponds to E_{L-1}, the next two to E_L and the last one to E_{L+1}. By using the Wick's theorem, E_L can be written as a determinant

$$E_L = \left\langle \prod_{j=1}^{L} \hat{b}_j^\dagger \hat{b}_j \right\rangle = \det \left[\left\langle \hat{b}_l^\dagger \hat{b}_j \right\rangle \right]_{l,j=1}^{L}. \quad (17)$$

Note that Eqs. (2) and (17) are equivalent. The calculation of E_n can be done by Fourier transforming the particle operators

$$\hat{c}_j = \frac{1}{\sqrt{N}} \sum_k e^{ijk} \hat{\mathcal{C}}_k \quad \text{and} \quad \hat{c}_j^\dagger = \frac{1}{\sqrt{N}} \sum_k e^{-ijk} \hat{\mathcal{C}}_k^\dagger, \quad (18)$$

where $k = 2\pi r/N$ with $-N_F/2 \leq r \leq N_F/2$. In this way, the average value $\left\langle \hat{b}_l^\dagger \hat{b}_j \right\rangle$ can be written as

$$\left\langle \hat{b}_l^\dagger \hat{b}_j \right\rangle = \delta_{l,j} - \frac{1}{N} \sum_k e^{ik(l-j)} n_k(\beta), \quad (19)$$

where $n_k(\beta) = 1/(1+\exp(-\beta\,\epsilon_k))$ is the average number of fermions in state k. The simplest case for the Eq. (19) is found at $T = 0$ because in that case the integral can be calculated exactly. At $T = 0$ we have

$$\left\langle \hat{b}_j^\dagger \hat{b}_j \right\rangle = 1 - \rho, \quad (20)$$

and

$$\left\langle \hat{b}_j^\dagger \hat{b}_l \right\rangle = \frac{\sin(2\pi(j-l)(1-\rho))}{\pi(j-l)}. \quad (21)$$

However, for $T > 0$ the integrals involved must be calculated numerically. To calculate $p^{(0)}(\ell)$, first Eqs. (17) and (19) (or (20) and (21) for $T = 0$) are used to calculate E_L. Then, Eq. (16) is used to evaluate $P^{(0)}(L)$. Finally, the scaled distribution, $p^{(0)}(\ell)$, is calculated from $P^{(0)}(L)$ using Eq. (9).

By definition, the next spacing distribution, $P^{(1)}(L)$ can be calculated from the following expression

$$\begin{aligned} P^{(1)}(L) &= \sum_{m=1}^{L-1} \mathcal{P}_{\mathcal{C}}(\downarrow \overbrace{\uparrow \cdots \uparrow\downarrow}^{m} \underbrace{\uparrow \cdots \uparrow\downarrow}_{L}) \\ &= \sum_{m=1}^{L-1} \mathcal{P}_{\mathcal{C}}(\bullet \overbrace{\circ \cdots \circ \bullet}^{m} \underbrace{\circ \cdots \circ \bullet}_{L}) \\ &= \sum_{m=1}^{L-1} \left[\left\langle \hat{c}_0^\dagger \hat{c}_0 \hat{\mathcal{O}}_1^{m-1}\, \hat{c}_m^\dagger \hat{c}_m \hat{\mathcal{O}}_{m+1}^{L-1} \hat{c}_L^\dagger \hat{c}_L \right\rangle \right], \end{aligned} \quad (22)$$

where we have defined $\hat{\mathcal{O}}_n^m = \prod_{j=n}^m \hat{b}_j^\dagger \hat{b}_j$. The sum in Eq. (22) considers that the inner particle can be at any position inside the gap. Writing the particle operators in terms of the corresponding hole operators we find

$$\begin{aligned} P^{(1)}(L) = \sum_{m=1}^{L-1} \Big[&\left\langle \hat{\mathcal{O}}_1^{m-1} \hat{\mathcal{O}}_{m+1}^{L-1} \right\rangle - \left\langle \hat{\mathcal{O}}_0^{m-1} \hat{\mathcal{O}}_{m+1}^{L-1} \right\rangle \\ &- \left\langle \hat{\mathcal{O}}_1^{L-1} \right\rangle + \left\langle \hat{\mathcal{O}}_0^{L-1} \right\rangle + \left\langle \hat{\mathcal{O}}_1^{L} \right\rangle - \left\langle \hat{\mathcal{O}}_0^{L} \right\rangle \\ &- \left\langle \hat{\mathcal{O}}_1^{m-1} \hat{\mathcal{O}}_{m+1}^{L} \right\rangle + \left\langle \hat{\mathcal{O}}_0^{m-1} \hat{\mathcal{O}}_{m+1}^{L} \right\rangle \Big]. \end{aligned} \quad (23)$$

All the terms in Eq. (16) can be interpreted as the probabilities associated with a given configuration. For instance,

$$\left\langle \hat{\mathcal{O}}_1^{L} \right\rangle = E_L = \mathcal{P}_{\mathcal{C}}(\overbrace{\circ \cdots \circ}^{L}), \quad (24)$$

and

$$\begin{aligned} \left\langle \hat{\mathcal{O}}_0^{m-1} \hat{\mathcal{O}}_{m+1}^{L} \right\rangle = &\ \mathcal{P}_{\mathcal{C}}(\overbrace{\circ \cdots \circ}^{m-1} \bullet \overbrace{\circ \cdots \circ}^{L-m}) \\ &+ \mathcal{P}_{\mathcal{C}}(\overbrace{\circ \cdots \circ}^{m-1} \circ \overbrace{\circ \cdots \circ}^{L-m}). \end{aligned} \quad (25)$$

Defining the second-order emptiness distribution, $E_{L,m}$, by

$$E_{L,m} = \left\langle \hat{\mathcal{O}}_1^{m-1} \hat{\mathcal{O}}_{m+1}^{L} \right\rangle, \quad (26)$$

one can write Eq. (23) in the following form

$$\begin{aligned} P^{(1)}(L) = \sum_{m=1}^{L-1} [&E_{L-2,m-1} - E_{L-1,m} - E_{L-1,m-1} \\ &+ E_{L,m} - E_{L+1} - E_{L-1} + 2E_L]. \end{aligned} \quad (27)$$

The determinantal representation of $E_{L,m}$ is given by

$$E_{L,m} = \det \left[\left\langle \hat{b}_{x_l}^\dagger \hat{b}_{x_j} \right\rangle \right]_{l,j=1}^{L}, \quad (28)$$

where $x_l = l$ for $l \leq m+1$ and $x_l = l+1$ for $l > m+1$. The evaluation of $p^{(1)}(\ell)$ is analogous to that of $p^{(0)}(\ell)$. First, we evaluate $E_{L,m}$ using Eq. (28), then Eqs. (27) and (9) are used to calculate $p^{(1)}(\ell)$.

Another distribution that can be used to describe the system is the probability of two consecutive domains with a total length L

$$\begin{aligned} Q(L) &= \sum_{l=1}^{L} \mathcal{P}_{\mathcal{C}}(\downarrow \overbrace{\uparrow\cdots\uparrow}^{l}\overbrace{\downarrow\cdots\downarrow}^{L-l}\uparrow) \\ &= \sum_{l=1}^{L} \mathcal{P}_{\mathcal{C}}(\bullet \overbrace{\circ\cdots\circ}^{l}\overbrace{\bullet\bullet\cdots\bullet\bullet}^{L-l}\circ) \\ &= \sum_{l=1}^{L} \left\langle \hat{c}_0^\dagger \hat{c}_0 \hat{\mathcal{O}}_1^l \hat{\mathcal{Q}}_{l+1}^L \hat{b}_{L+1}^\dagger \hat{b}_{L+1} \right\rangle, \end{aligned} \tag{29}$$

where $\hat{\mathcal{Q}}_{l+1}^L = \prod_{j=l+1}^{L} \hat{c}_j^\dagger \hat{c}_j$. Unfortunately, $Q(L)$ cannot be evaluated as easily as the distributions $p^{(0)}(\ell)$ and $p^{(1)}(\ell)$ except for the trivial high-temperature regime. In the next section we use the spacing distributions to describe the magnetic behavior of the XX spin chain.

4. Results

As explained in Section II, at $T = 0$ and $h > 0.5$ we have $\mathcal{M} = 1$ in such way that there is a single domain formed by spins parallel to the magnetic field. In this case, $P^{(0)}(L) = \delta_{L,N}$. For arbitrary values of T and $h = 0$, the domain distribution of spins up and down are equivalent.

At high temperatures, it is reasonable to expect that the spins behavior is dominated by the thermal fluctuations. In this regime it is possible to neglect the correlations between adjacent sites. Thus, Eq. (15) can be written as

$$\begin{aligned} P^{(0)}(L) &\approx \left\langle \hat{c}_0^\dagger \hat{c}_0 \right\rangle \prod_{j=1}^{L-1} \left\langle \hat{b}_j^\dagger \hat{b}_j \right\rangle \left\langle \hat{c}_L^\dagger \hat{c}_L \right\rangle \\ &= \rho^2 (1-\rho)^L, \end{aligned} \tag{30}$$

where we have used $\left\langle \hat{c}_j^\dagger \hat{c}_j \right\rangle = \rho$ and $\left\langle \hat{b}_j^\dagger \hat{b}_j \right\rangle = 1 - \rho$. Similarly, the probability $Q(L)$ can be approximated as follows

$$\begin{aligned} Q(L) &\approx (1-\rho) \sum_{l=1}^{L-1} \rho^l (1-\rho)^{L-l} \rho \\ &= \frac{(\rho-1)\rho\left((\rho-1)\rho^L + \rho(1-\rho)^L\right)}{2\rho - 1}. \end{aligned} \tag{31}$$

As seen in Fig. (5), Eqs. (30) and (31) reproduce $P^{(0)}(L)$ and $Q(L)$ for $h = 0$ and $T = 10$. However, for low temperatures, quantum fluctuations are relevant, and the spacing distributions cannot be approximated by Eqs. (30) and (31); see dotted-lines in Fig. (5). In fact, for high temperatures the spacing distributions decay monotonically which does not occur for low temperatures, indicating that consecutive domains are correlated. At $T = 10$ the most probable length of a domain is one; thus it is very likely to find two consecutive spins in opposite directions. For $T = 0.0025$ the most probable length is two due the formation of dimers.

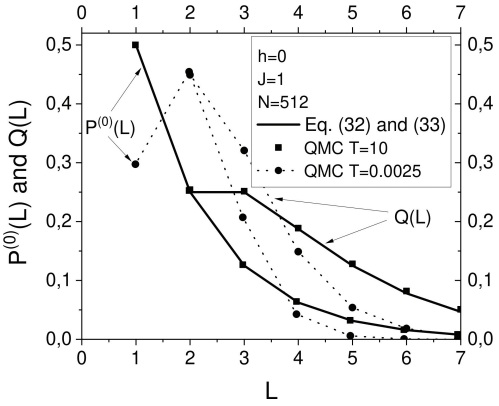

Figure 5: Spacing distributions for $T = 0.0025$ and $T = 10$ with $h = 0$. For high temperatures ($k_B\,T \gg J - 2\,h$) thermal fluctuations dominate and the correlations between adjacent sites are negligible. However, Eqs. (30) and (31) do not describe the behavior of the system for low temperatures ($k_B\,T \ll J - 2\,h$).

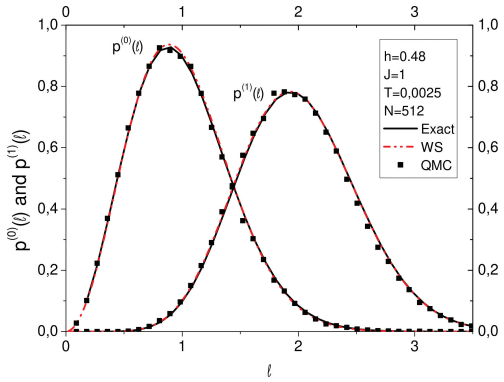

(a) Spacing distributions at $T = 0.0025$ and $h = 0.48$.

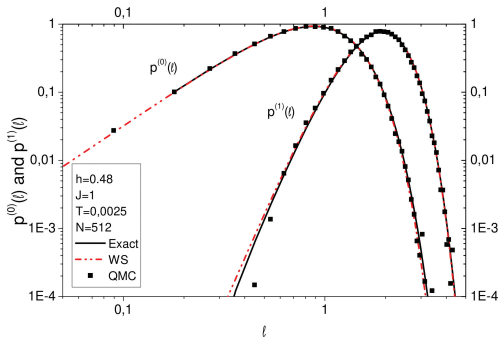

(b) Log-log replot of panel (a).

Figure 6: Spacing distributions as functions of the scaled distance ℓ for $T = 0.0025$. Note that, for the parameters selected, $\beta(J - 2h) = 16$. Therefore, the system is in the low temperature regime. As expected, the exact results coincide with the numerical results obtained from the quantum Monte Carlo simulations. The EWS provides and excellent approximation for $p^{(0)}(\ell)$ and $p^{(1)}(\ell)$, even for small and large values of ℓ.

 DOI: https://doi.org/10.1590/1806-9126-RBEF-2023-0019

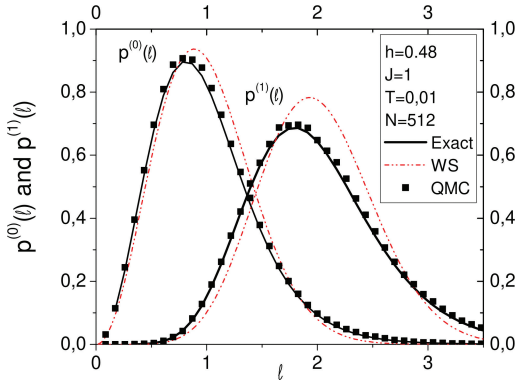

(a) Spacing distributions at $T = 0.01$ and $h = 0.48$.

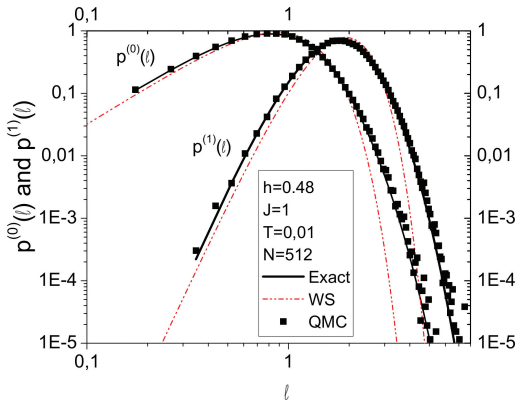

(b) In a Log-log replot of panel (a) it is easier to see that the behavior for small values of ℓ remains unaltered.

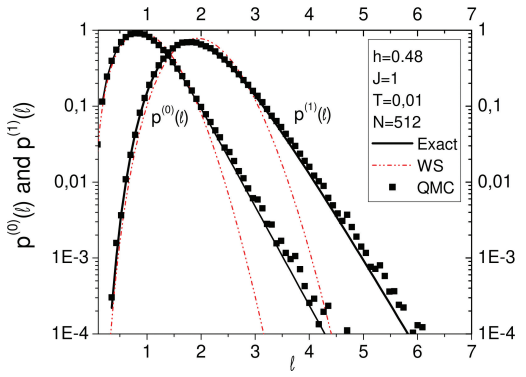

(c) On a log-linear replot, it becomes evident that the behavior for large values of ℓ changes from Gaussian to exponential.

Figure 7: Plots of spacing distributions $p^{(0)}(\ell)$ and $p^{(1)}(\ell)$ with replots to highlight the behavior at small and at large ℓ. At $T = 0.01$, the spacing distributions given by the QMC simulations deviate from the EWS but still coincide with the exact results. In this case, the parameters were selected in such way that $\beta(J - 2h) = 4$. Therefore, the energy associated with thermal fluctuations is comparable with the interaction energy and the system is not in the low temperature regime.

However, the most interesting behavior is found for values of h smaller than but close to $J/2$. In this region, the number of fermions is nearly to zero, i.e., domains of spins parallel to h form. The domain-length distribution is given by the inter-particle distribution $p^{(0)}(\ell)$. The probability to find two consecutive domains of up spins separated by a single down spin is given by $p^{(1)}(\ell)$. The behavior of the first two spacing distributions for $h = 0.48$, $J = 1$ and $T = 0.0025$ is shown in Fig. (6). The continuous lines correspond to the analytic expressions given by Eqs. (16) and (27), dots to the QMC simulations and the dash-dotted line to the extended Wigner surmise (EWS) with $\beta = 2$, see Appendix C. Given the complexity of the analytical expressions for the spacing distributions $p^{(0)}(\ell)$ and $p^{(1)}(\ell)$ it is convenient to use the approximate expressions provided by the EWS; see Appendix C. Note the excellent agreement between the QMC results and the ones given by Eqs. (16) and (27). The logarithmic scale used in Fig. 6 (b) highlights the behavior of the distribution for small and large values of ℓ.

As T increases, the thermal fluctuations randomize the system, and the right tail of the distribution becomes exponential rather than Gaussian, see Fig. (7). However, the behavior for small values of ℓ remains unchanged.

5. Conclusions

The XX spin chain is an excellent illustrative example of the rich behavior that can be found in interacting many-particle systems. This system can be solved analytically but can be used also to illustrate the numerical methods such as the QMC. The domain distributions can be easily obtained by using QMC from the configurations of spins generated in the simulation. The spacing distributions are not usually calculated in courses of quantum statistical mechanics but as shown, they are very revealing, allowing us to describe the magnetic behavior of the spin chain in several regimes. The most interesting behavior is found for $2h$ slightly less than J. Thermal fluctuations change the functional form of the right tail of $p^{(0)}(\ell)$ and $p^{(1)}(\ell)$. At $T = 0$ the spacing distribution has Gaussian right tails but for $T > 0$ they are exponential. The left tail of the distributions is not affected by thermal fluctuations. For large T the correlations between adjacent sites can be neglected, and the spacing distributions can be calculated easily. In fact, the probability to find two or more consecutive domains can be obtained by using the independent-interval approximation, where the required distribution is written in terms of the convolution of single-domain distributions. This approach can also be used to illustrate how the IPDF method can be represented using second quantization formalism; thus, it can be used to study reaction-diffusion systems.

Acknowledgments

DLG is thankful for support from Vicerrectoría de Investigaciones, Universidad del Valle (Colombia).

Supplementary Material

The following online material is available for this article:
Appendix A: Jordan-Wigner transformation
Appendix B: Calculation of $Z_N(\beta)$
Appendix C: Extended Wigner surmise

References

[1] L.E. Reichl, *A Modern Course in Statistical Physics* (Wiley-VCH, Weinheim, 2016), 4 ed.

[2] M. Kardar, *Statistical Physics of Particle* (Cambridge University Press, Cambridge, 2007), 1 ed.

[3] R.K. Pathria and P. Beale, *Statistical Mechanics* (Academic Press, Amsterdam, 2011), 3 ed.

[4] K. Huang, *Statistical Mechanics* (John Wiley & Sons, New York, 1987), 2 ed.

[5] L.D. Landau and E.M. Lifschitz, *Statistical Physics – part 1* (Pergamon Press, Oxford, 1980), 3 ed.

[6] F. Reif, *Fundamentals of Statistical and Thermal Physics* (McGraw-Hill, New York, 1965).

[7] F. Schwabl, *Statistical Mechanics* (Springer, Berlin, 2006), 2 ed.

[8] L. Peliti, *Statistical Mechanics in a Nutshell* (Princeton University Press, Princeton, 2011).

[9] T. Giamarchi, *Quantum Physics in One Dimension* (Clarendon Press, Oxford, 2004).

[10] K. Binder and D. Heermann, *Monte Carlo Simulation in Statistical Physics* (Springer-Verlag Berlin Heidelberg, Berlin, 2010).

[11] F. Franchini, *An Introduction to Integrable Techniques for One-Dimensional Quantum Systems* (Springer, Cham, 2017), 1 ed.

[12] D.A. McQuarrie, *Statistical Mechanics* (Harper & Row, New York, 1975).

[13] D. Chandler, *Introduction to Modern Statistical Mechanics* (Oxford University Press, Oxford, 1987).

[14] M. Takahashi, *Thermodynamics of One-Dimensional Solvable Models* (Cambridge University Press, Cambridge, 1999).

[15] M. Shiroishi, M. Takahashi and Y. Nishiyama, Phys. Soc. Jpn. **70**, 3535 (2001).

[16] M. Shiroishi and M. Takahashi, J. Phys. Soc. Jpn. **74**, 47 (2005).

[17] F. Ares and J. Viti, J. Stat. Mech.: Theory and Experiment. **2020**, 013105 (2020).

[18] V.E. Korepin, A.G. Izergin, F.H.L. Essler and D.B. Uglov, Phys. Lett. A **190**, 182 (1994).

[19] A.G. Abanov and F. Franchini, Phys. Lett. A **316**, 342 (2003).

[20] A.W. Sandvik, Phys. Rev. B **59**, R14157(R) (1999).

[21] O.F. Syljuasen and A.W. Sandvik, Phys. Rev. E **66**, 046701 (2002).

[22] A.W. Sandvik, in: *2012 Theory Winter School. National High Magnetic Field Laboratory* (Tallahassee, 2012).

[23] D. ben-Avraham, Modern Phys. Lett. B **9**, 895 (1995).

[24] D. ben-Avraham and S. Havlin, *Diffusion and Reactions in Fractals and Disordered Systems* (Cambridge University Press, Cambridge, 2000).

[25] D.F. Jaramillo, G. Téllez, D.L. González and T.L. Einstein, Phys. Rev. E **87**, 052405 (2013).

[26] A.Y. Abul-Magd and M.H. Simbel, Phys. Rev. E **60**, 5371 (1999).

[27] M.L. Mehta, *Random Matrices* (Academic Press, San Diego, 2004), 3 ed.

[28] D.L. González and G. Téllez, Phys. Rev. E **76**, 011126 (2007).

[29] D.L. González, A. Pimpinelli and T.L. Einstein, Phys. Rev. E **85**, 011151 (2012).

[30] B. Joós, T.L. Einstein and N.C. Bartelt, Phys. Rev. B **43**, 8153 (1991).

[31] Z.N.C. Ha, *Quantum Many-Body Systems in One Dimension* (World Scientific, Singapore, 1996).

[32] J.B. Parkinson and D.J.J. Farnell, *An Introduction to Quantum Spin Systems* (Springer, Cham, 2010).

[33] W.J. Caspers, *Spin Systems* (World Scientific, Singapore, 1989).

[34] P. Jordan and E. Wigner, Z. Phys. **47**, 631 (1928).

[35] D.F. Jaramillo, G. Téllez, D.L. González and T.L. Einstein, Phys. Rev. E **87**, 052405 (2013).

[36] D.L. González and G. Téllez, J. Stat. Phys. **132**, 187 (2008).